Chitosan Supported onto Agave Fiber—Postconsumer HDPE Composites for Cr(VI) Adsorption

I&EC research
Industrial & Engineering Chemistry Research

ARTICLE

pubs.acs.org/IECR

Chitosan Supported onto Agave Fiber—Postconsumer HDPE Composites for Cr(VI) Adsorption

A. Alejandra Pérez-Fonseca, Cesar Gómez, Haydeé Dávila, and Rubén González-Núñez*

Departamento de Ingeniería Química, Universidad de Guadalajara, 44430 Jalisco, México

Jorge R. Robledo-Ortíz

Departamento de Madera, Celulosa y Papel, Universidad de Guadalajara, 45510 Jalisco, México

Milton O. Vázquez-Lepe and Alberto Herrera-Gómez

CINVESTAV-IPN, 76230 Querétaro, México

ABSTRACT: Composites of high-density polyethylene and agave fibers coated with chitosan were used as adsorbent for Cr(VI). The adsorptions were made in batch and continuous systems. Different kinetic models were used to characterize the batch adsorption and to determine the adsorption capacity of the compound. To test the composite regeneration/reuse capability, the chromium content in the composite material was desorbed using different acids. The coated composites were characterized by scanning electron microscopy (SEM), attenuated total reflectance infrared spectroscopy (ATR-IR), and X-ray photoelectric spectroscopy (XPS). From the results it was found that the composite has a maximum adsorption capacity of 200 mg Cr(VI)/g of chitosan at pH 4. Sulfuric acid proved to be a good desorbent of Cr(VI), allowing the material to be reused while keeping its adsorption properties. Finally, the results showed that the continuous system has higher sorption capacity than the batch system; it was determined that the system needs a minimum retention time of 20 min in order to use the material in the treatment of contaminated effluents.

1. INTRODUCTION

Nowadays, water pollution is a crucial issue of concern. Heavy metals are of particular concern due to their toxicity and carcinogenic character.[1,2] Waste streams from industries, such as chrome plating and processing units, tanneries, and electronic device manufacturing facilities, contain significant quantities of chromium and other trace metals.[3] In fact, chromium is listed as a priority pollutant and carcinogen by the United States Environmental Protection Agency (EPA).

Several methods such as chemical precipitation, oxidation/reduction, mechanical filtration, ion exchange, membrane separation, and carbon adsorption are among the variety of treatment processes widely used for the removal of toxic heavy metals from waste streams.[4−6]

Two stable oxidation states of chromium persist in the environment, Cr(III) and Cr(VI), which have contrasting toxicities, mobilities, and bioavailability. Whereas Cr(III) is essential in human nutrition, most of the hexavalent compounds are toxic; several of them can even cause lung cancer. Cr(VI) moves readily through soils and aquatic environments and is a strong oxidizing agent capable of being absorbed through the skin.[7,8]

Natural materials that are available in large quantities or certain wastes from agricultural operations may have the potential to be used as low-cost sorbents, since they represent widely available and environmentally friendly unused resources.[8,9] Materials such as fly ash, silica gel, zeolites, lignin, seaweed, wool wastes, agricultural wastes, clay materials, and sugar cane bagasse, etc., have been extensively investigated for the removal of pollutants from aqueous streams, especially for heavy metals like Cd(II), Cr(III), Cr(VI), Hg(II), and Pb (II).

Chitin is a natural polymer found abundantly in the exoskeletons of insects, shells of crustaceans, and fungal cell walls. Chitosan is obtained from an alkaline deacetylation procedure of the chitin.[10,11] The excellent adsorption characteristics of chitosan are due to the large number of hydroxyl groups, primary amine groups with high activity at the adsorption sites, and the flexible structure of the polymer chain that allows the proper configuration for the formation of chitosan−metal complexes.[12,13]

Although amine and hydroxyl groups in chitosan are mainly responsible for the adsorption of metal ions, these active binding sites are not readily available for sorption when chitosan is in a gel or in its natural form due to low porosity.[3,14] Using pure chitosan as an adsorbent has some disadvantages such as low surface area, high cost, and poor chemical and mechanical properties.[15] Physical or chemical chitosan modifications have been studied as an alternative in adsorption processes; to improve chitosan adsorption ability cross-linking reagents have been used. On the other hand, chitosan composites have been developed to adsorb heavy metals from wastewater and have been proven to have

Special Issue: AMIDIQ 2011

Received: June 9, 2011
Accepted: October 13, 2011
Revised: October 12, 2011
Published: October 13, 2011

dx.doi.org/10.1021/ie201242x | *Ind. Eng. Chem. Res.* 2012, 51, 5939–5946

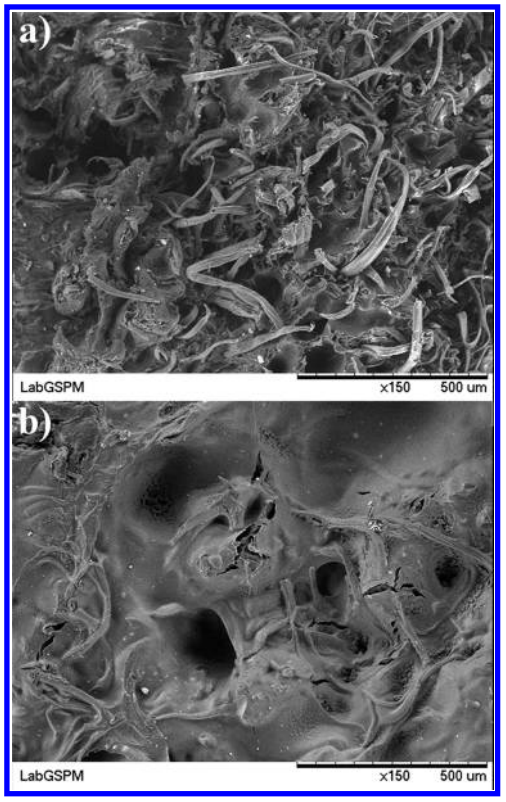

Figure 1. SEM micrographs of (a) composite and (b) chitosan-coated composite.

better adsorption capacity and resistance to acidic environments.[16]

In this sense, a composite of high-density polyethylene and agave fiber was used as support for chitosan, and this system was subsequently used in batch and continuous systems to adsorb Cr(VI) from aqueous solutions.

2. MATERIALS AND METHODS

2.1. Materials. HDPE (PADMEX 65050, PEMEX, Mexico) with a melt index of 5 g/10 min and a density of 0.9665 g/cm^3 was used as a matrix. The agave fibers used were residues from a local tequila company. The chemical blowing agent was azodicarbonamide (ACA) (Sigma−Aldrich, USA). Zinc oxide (Sigma−Aldrich, USA) was used as catalyst. Industrial-grade powder chitosan (America Alimentos, Mexico) with 95% deacetylation (determined by infrared spectroscopy analysis) was used. Potassium dichromate, acetic acid, and 1,5 diphenylcarbazide were from Sigma Aldrich, USA. Sodium hydroxide was from Golden Bell, México, and nitric, sulfuric, and hydrochloric acids were from J. T. Baker, Mexico.

2.2. Sorbent Preparation. The composite was produced using 70% HDPE and 30% agave fiber (w/w); the HDPE was previously mixed with 1% ACA and 0.1% ZnO (w/w). Prior to the mixing, the agave fiber was cleaned as follows: a sifting was made to eliminate the solids, later the pithy fibers were soaked in a container with tap water for 24 h to hydrate the fibers and to facilitate pith separation. This separation was made in a Sprout-Waldron refiner (D2A509NH) with two 30-cm-diameter discs, one fixed and the other rotating at 1770 rpm. Using centrifugation, the excess water in the fibers was eliminated. Finally, the

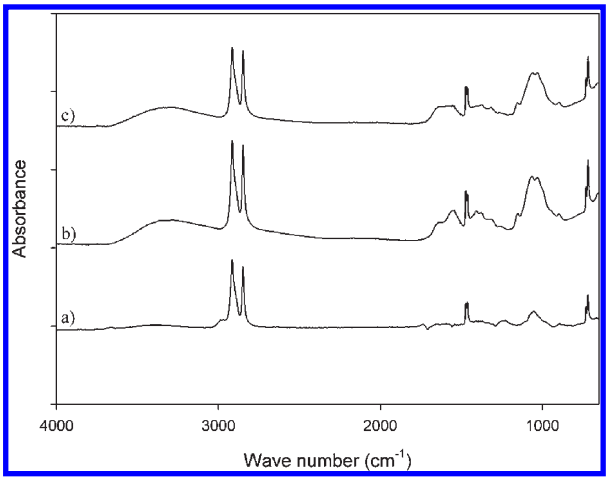

Figure 2. FTIR-ATR spectra of (a) C, (b) CCC, and (c) CCC-Cr.

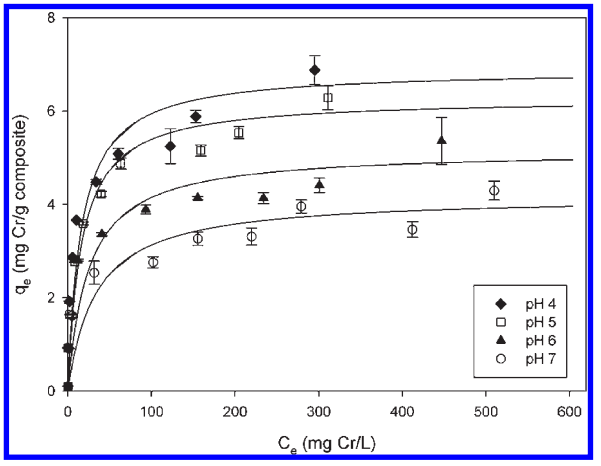

Figure 3. Cr(VI) adsorption isotherms as function of pH. The continuous lines are predictions by the Langmuir model.

fibers were air-dried and milled. Afterward, the composites were extruded and foamed in a double-screw extruder Leistritz micro 26 GL/GG-36D. The temperature profile in the extruder was 90/120/140/150/160/166/173/178/170 °C with a screw speed of 90 rpm. After extrusion, the material was pelletized. The size of obtained pellets was 3.06 ± 0.2 mm diameter and 3.49 ± 0.2 mm length with an average density of 0.62 g/cm^3. The composite pellets were treated with a chemical process to incorporate chitosan.[17] This treatment consisted of composite immersion in an alkali bath of 10 wt % NaOH solution for 24 h, followed by an immersion in a 2% v/v acetic acid solution. The material was dried in a solar dryer for one day. Afterward, 100 g of dried pellets was immersed in 500 mL of chitosan solution (2% wt) previously dissolved in 2% v/v acetic acid. The material was placed in a solar dryer for solvent evaporation and to promote the incorporation of chitosan as a film onto the pellet surface. The pellets coated with chitosan were washed with distilled water to remove the excess chitosan until the solution pH remained at 7. Finally the composite-chitosan pellets were dried in the solar dryer before their use.

2.3. Sorbent Characterization. The surface morphology of the sorbent was studied via scanning electron microscopy (TM-1000 Tabletop microscope, Hitachi High-Technologies Inc., Japan).

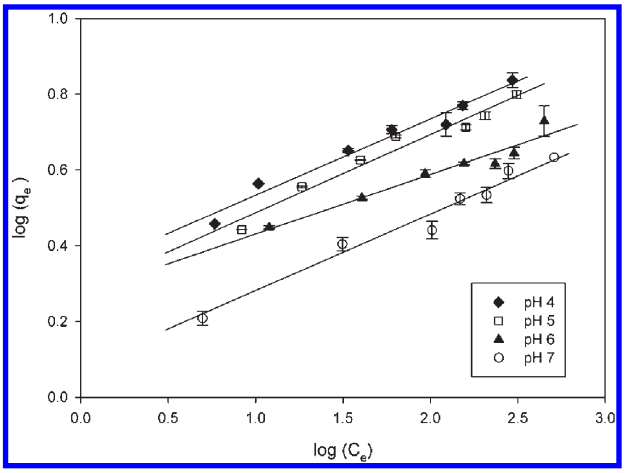

Figure 4. Cr(VI) adsorption isotherms as function of pH. The continuous lines are predictions by the Freundlich model.

Table 1. Langmuir and Freundlich Parameters

	Langmuir model			Freundlich model		
pH	q_{max} (mg g^{-1})	b (L mg^{-1})	R^2	$1/n$	K_f	R^2
4	6.887	0.063	0.9846	0.2014	1.3938	0.969
5	6.269	0.062	0.9896	0.2067	1.3237	0.9636
6	5.159	0.041	0.9776	0.1572	1.315	0.9409
7	4.175	0.03	0.9767	0.202	1.0829	0.9136

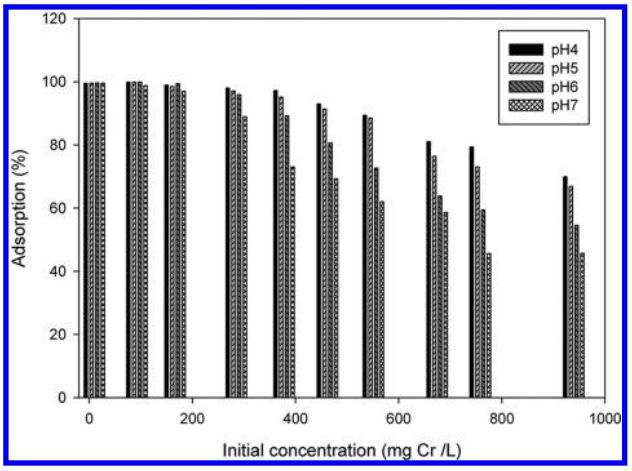

Figure 5. Cr(VI) adsorption as function of pH and initial concentration.

The amount of chitosan incorporated to the composite surface was measured by weight difference. Additionally, the treated composite was characterized with Fourier transform infrared-attenuated total reflectance (FTIR-ATR) in a Perkin-Elmer Spectrum 100 FTIR Spectrometer with a Universal ATR accessory.

2.4. Equilibrium Adsorption Isotherms. Equilibrium adsorption isotherms were conducted in batch systems using potassium dichromate solutions prepared with DI water, with initial Cr(VI) concentrations between 10 and 1000 mg/L. The pH of the solutions was varied between 4 and 7 (adding HCl or NaOH as needed) in order to study pH values similar to those presented in typical Cr-polluted rivers[18,19] and to evaluate its effect on the adsorption process. The experiments were carried out in 15-mL

Table 2. Kinetic Parameters for Pseudo-Second-Order Equation

C_0 (mg L^{-1})	q_e (mg g^{-1})	K (g mg^{-1} min^{-1})	R
194	55.50	2.63	0.999
292	81.88	0.86	0.998
481	126.42	0.09	0.998
647	165.27	0.24	0.999

glass vials by contacting 1 g of prepared composite with 10 mL of chromium solution for 6 h (time to reach equilibrium), in a reciprocal Barnstead Shke5000-7 shaker bed at 25 °C and a 150 rpm agitation. After reaching the equilibrium the sorbent was filtered from the solution and the filtrate were analyzed for Cr(VI). All the experiments were performed in triplicate. The amount of the metal adsorbed (mg) per unit of sorbent mass q_e was obtained using eq 1.

$$q_e = \frac{(C_0 - C_e)V}{M} \quad (1)$$

where C_0 and C_e are initial and equilibrium concentration of Cr(VI) in the solution, respectively (mg L^{-1}), M is the dry mass of sorbent (g), and V is the solution volume (L). The equilibrium isotherms were fitted to the Langmuir and Freundlich models, given by eqs 2 and 3, respectively.

$$q_e = \frac{q_{max} b C_e}{1 + bC_e} \quad (2)$$

$$q_e = K_f C_e^{1/n} \quad (3)$$

where q_{max} is the maximum amount adsorbed within a monolayer (mg g^{-1}) and b is the Langmuir dissociation constant which is related to the adsorption energy. K_f and $1/n$ are the Freundlich constants that indicate adsorption capacity and adsorption intensity, respectively.

To investigate the adsorption mechanism, the models of Lagergren and the pseudo-second-order were used to find the kinetic parameters. The first-order equation of Lagergren is expressed as

$$\log(q_e - q) = \log q_e - \frac{k_{s1}}{2.303} t \quad (4)$$

The pseudo-second-order equation is

$$\frac{t}{q} = \frac{1}{K q_e^2} + \frac{t}{q_e} \quad (5)$$

where q_e and q are the amount of metal sorbed per unit weight of sorbent at equilibrium and at any time t, respectively (mg g^{-1}), k_{s1} (min^{-1}) and K (g mg^{-1} min^{-1}) are the rate constants of Lagergren and pseudo-second-order sorption.

2.5. Measurement of Chromium Ions. The hexavalent chromium concentration was determined colorimetrically[20] by measuring the intensity of the red−violet complex formed by the reaction of Cr(VI) with 1,5-diphenylcarbazide in acidic media. A UV−vis spectrometer (Agilent 8453) was used to obtain the absorbance of formed complex at 540 nm. Sample concentrations were determined using a calibration curve from standard Cr(VI) solutions.

2.6. Batch Desorption Experiments. To determine the reusability of the sorbents, consecutive adsorption−desorption cycles were repeated. Cr(VI) was desorbed with 0.1 M HCl, 0.1 M H_2SO_4,

dx.doi.org/10.1021/ie201242x |Ind. Eng. Chem. Res. 2012, 51, 5939–5946

Table 3. Chromium Desorbed from Composite by Different Solutions

solution 0.1 M	pH	desorption %
NaOH	12.1	44.5
H_2SO_4	1.5	27.3
HNO_3	1.4	7.5
HCl	1.2	2.2

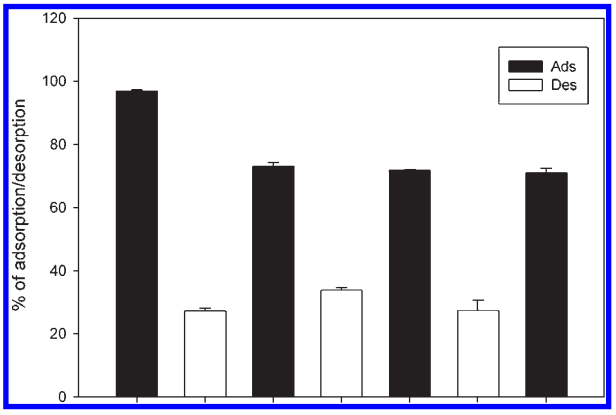

Figure 6. Adsorption and desorption cycles of chromium using H_2SO_4.

0.1 M NaOH, and 0.1 M HNO_3. Adsorption cycles were conducted using solutions of 300 mg/L with the same conditions used in batch experiments: 1 g of material was added to 10 mL of solution for 4 h. After adsorption time, the material was washed with DI water. The material loaded with chromium was placed in 10 mL of desorption medium and stirred at 150 rpm for 1 h at 25 °C. This adsorption procedure was repeated four times and the desorption was repeated three times. After desorption, the sorbent was washed with distilled water and used in the succeeding cycle. The amount of chromium desorbed was calculated from the amount of chromium adsorbed on the adsorbent and the final chromium concentration in the desorbed solution.

2.7. XPS Studies. XPS was used to determine the chemical states of the functional groups on the composite surface. The samples for XPS analysis were taken from batch experiments. XPS data were obtained with an XPS110 electron analyzer ThermoElectron (East Grinstead, UK) instrument with monochromatic Al X-rays (hv =1486.7 eV) at 180 W with an electron takeoff angle of 90°. The calibration of the binding energy of the spectra was performed with the C1s peak of the carbon due to atmospheric contamination, which was at 284.8 eV. The XPS peaks were decomposed into subcomponents with the software AAnalyzer v 1.1. The spectra were measured on (a) composite *C*, (b) composite coated with chitosan *CCC*, and (c) composite coated with chitosan and loaded with chromium *CCC-Cr*. Other details can be found elsewhere.[17]

2.8. Column Adsorption Experiments. Column studies were conducted in a glass column of 1.5 cm internal diameter by 60 cm length at 25 ± 3 °C.

The column was fully packed using 36.2 g of sorbent material (60 cm of bed height). The Cr solutions were passed through the columns at a flow rate of 2 mL min^{-1}; the initial inlet concentration was 99.7 mg/L. Samples were taken at different time intervals and analyzed colorimetrically (as pointed out in Section 2.5). Column studies were concluded when the adsorbent material reached saturation.

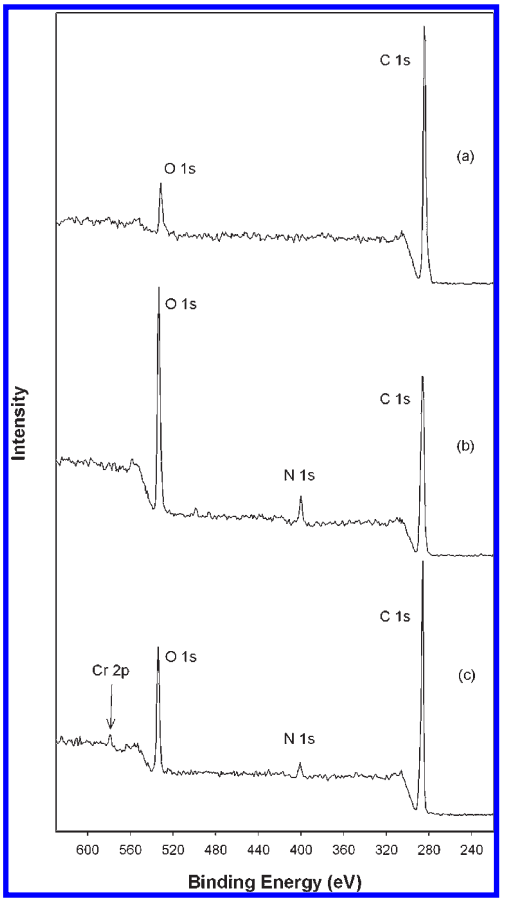

Figure 7. XPS wide-scan spectra of (a) composite C, (b) CCC, and (c) CCC-Cr.

3. RESULTS AND DISCUSSION

3.1. Composite Micrographs. Changes in the composite surface are presented in Figure 1. Micrographs of the chitosan-free composite (left) and the composite coated with chitosan (right) are presented; a complete coverage of the composite surface by chitosan is observed. The chemical treatment made possible the exposure of agave fibers on the composite; because of that, a better incorporation of chitosan was achieved,[17] the net amount of chitosan coating the sorbent was 3.31% wt/wt.

3.2. FTIR Analysis. FTIR analyses were used to investigate interactions between metal ions and chelating groups of the composite, and spectra of (a) C, (b) CCC, and (c) CCC-Cr are shown in Figure 2. The samples showed two peaks at 2900 and 2800 cm^{-1}, assigned to C−H stretching of CH_2 groups of the polymeric matrix, another band due to the C−H bending of CH_2 groups of polyethylene. A peak at 1030 cm^{-1} is related to vibrations of −CO groups from cellulose.[21] There is a band at 3350 cm^{-1} which corresponds to −OH and −NH groups from cellulose and chitosan. The vibration of −NH groups from chitosan appears between[22] 1400 and 1660 cm^{-1}, in spectra (b) and (c) there is a band at 1521 cm^{-1} assigned to deformation of $-NH^{3+}$ group.[23] The presence of metal ions caused changes in this band, which suggests the amine group interaction with metal ions.

3.3. Adsorption Isotherms. Batch adsorption experiments indicate that removal of Cr (VI) is faster at the first hour and it reached equilibrium at 6 hours. Langmuir and Freundlich are the

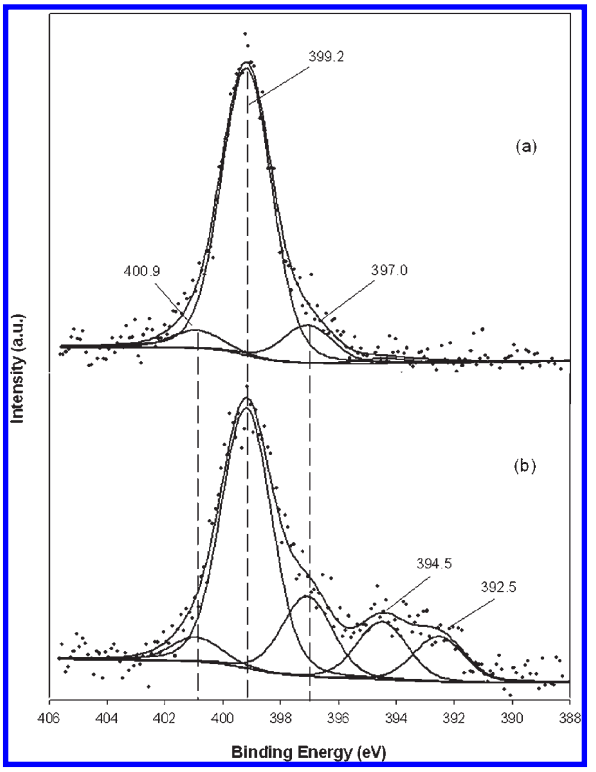

Figure 8. N1s core-level XPS spectra of (a) CCC and (b) CCC-Cr.

most widely referred models for isotherms description; Figures 3 and 4 present the isotherms, respectively. The parameters of Langmuir and Freundlich models are shown in Table 1. For the full range of concentrations (10−1000 mg/L) the Langmuir model has better correlation than Freundlich's. Nevertheless, for concentrations above 200 mg/L the fitting of the experimental data to Freundlich is better as observed in Figure 4. Adsorption capacity increases as the initial chromium concentration is increased.

The pH is an important parameter on the adsorption process. Vicent and Guibal[24] suggested that the pH should be maintained below 4.5. Figure 5 shows the percentage of Cr(VI) adsorbed for several initial concentrations. It can be seen in the figure that for concentrations up to around 200 mg/L almost 100% of the metal is adsorbed, and beyond this concentration the percentage of Cr sorbed decreases for all the pH conditions studied. Chromium uptake is higher at low pH because the acidic media provides an electrostatic balance between amine sites and metal ions.[10] At neutral pH, about 50% of total amine groups remain protonated and theoretically available for the sorption of metal anions. However, the existence of free amine groups may cause direct chelation of metal cations (which may coexist with anionic species, depending on the speciation of the metal). As the pH decreases, the protonation of amine groups increases, together with the adsorption efficiency.[25] Nevertheless, as mentioned before, in this study a pH range of 4−7 was used in order to obtain conditions comparable to those in polluted natural effluents.

The maximum adsorption capacity observed for the composite was 200.8 mg Cr(VI)/g of chitosan at pH 4. Maximum values reported in the literature are 78 mg for unsupported chitosan,[26] 153.8 mg for chitosan-coated alumina,[5] and 325 mg for glutaraldehyde cross-linked xanthated chitosan.[27] The value obtained in the present study (200.8 mg Cr (VI)/g of chitosan) is considerably

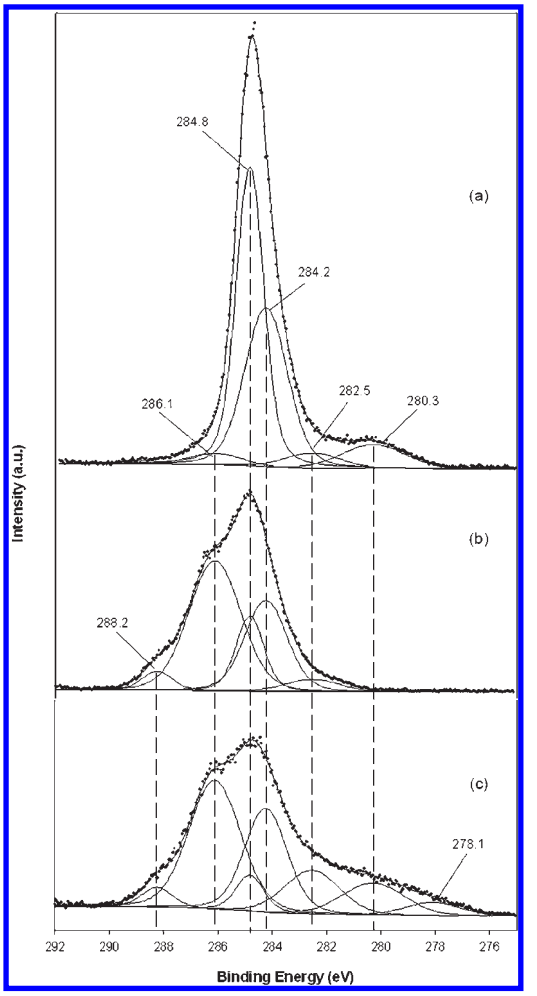

Figure 9. C1s core-level XPS spectra of (a) composite C, (b) CCC, and (c) CCC-Cr.

greater than unsupported chitosan values. Active sites of chitosan are not available in its natural form; when acid treatments are applied to chitosan, a protonation of amine groups occurs increasing the adsorption capacity.[25] The value is also higher than the maximum adsorption with chitosan-coated alumina, and in the case of cross-linked chitosan, although our value is lower, some important disadvantages are reported in the literature such as toxicity and complex obtaining procedures.[28]

3.4. Kinetic Analysis. The experimental results were fitted to linearized forms of Lagergren first- and pseudo-second-order model equations.[6] The first-order model did not fit to the experimental data (data not shown). According to Sag and Aktay,[2] the pseudo-second-order model (eq 5) is the most recommended for this kind of adsorption, because it is based on the sorption capacity of the solid phase and is in agreement with a chemisorption mechanism as the rate-controlling step.[16,29]

The parameters obtained are shown in Table 2. The four sets of experiments at different concentrations used showed a good correlation for this model.

3.5. Desorption of Chromium. The amounts of chromium desorbed using HCl, H_2SO_4, NaOH, and HNO_3 are displayed in Table 3. The greater amount of chromium desorbed was obtained when sodium hydroxide was used. NaOH is one of the most common desorbents,[5,8,24] nevertheless in this study the composite desorbed in NaOH solutions loses its adsorption ability.

dx.doi.org/10.1021/ie201242x |*Ind. Eng. Chem. Res.* 2012, 51, 5939–5946

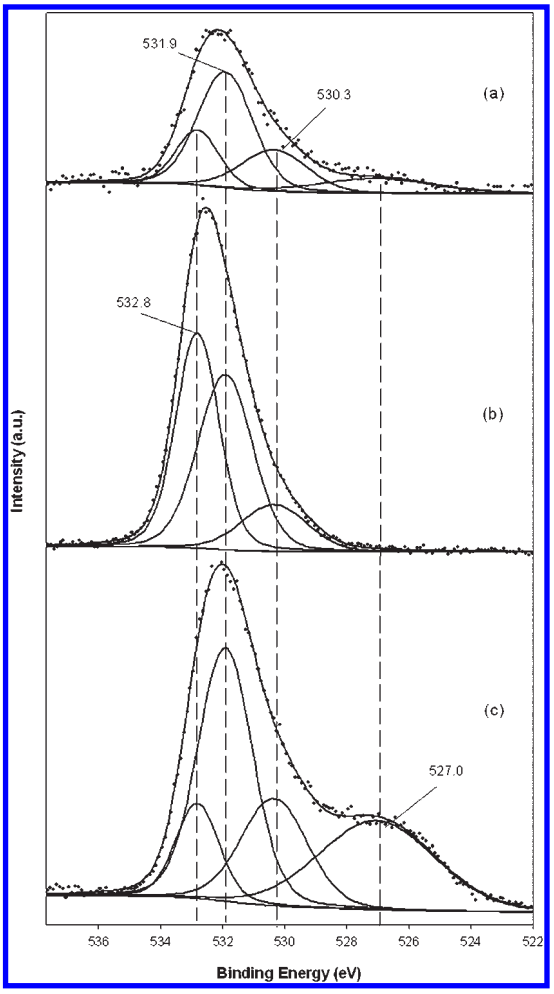

Figure 10. O1s core-level XPS spectra of (a) composite C, (b) CCC, and (c) CCC-Cr.

On the other hand, HCl and HNO_3 solubilized chitosan, but H_2SO_4 did not,[30] thus the sorption−desorption cycles were run using only H_2SO_4, this acid desorbs 27.26% of the Cr(VI). Four cycles of adsorption and three cycles of desorption are shown in Figure 6, where it can be seen that the behavior is similar and also that the material keeps adsorbing chromium.

3.6. XPS Analysis. The composites were studied by XPS before and after contact in chromium solution to determinate the chemical states of the surface. Also, it was interesting to investigate the interaction between the metal and the functional groups of the composite. Figure 7 shows the wide-scan XPS spectra for C (Figure 7a), CCC (Figure 7b), and CCC-Cr composite with chromium adsorbed (Figure 7c). Based on composite (C), the predominant peaks were O1s (531.9 eV) and C1s (284.8 eV). The presence of a new peak 399.2 eV at Figure 7b corresponds to N1s from amino group of chitosan. Figure 7c shows a slightly and significant peak characteristic of the Cr2p peak around 576 eV.

Figure 8 shows the high-resolution N1s core-level spectra resolved into individual components for samples CCC (Figure 8a) and CCC-Cr (Figure 8b). In the case of sample CCC, the required three peaks for the curve fit, one at 399.2 eV corresponding to the primary amine ($-NH_2$), other low intensity peak at 400.9 eV corresponding to the protonated ammonium ion ($-NH_3^+$), and other low intensity peak

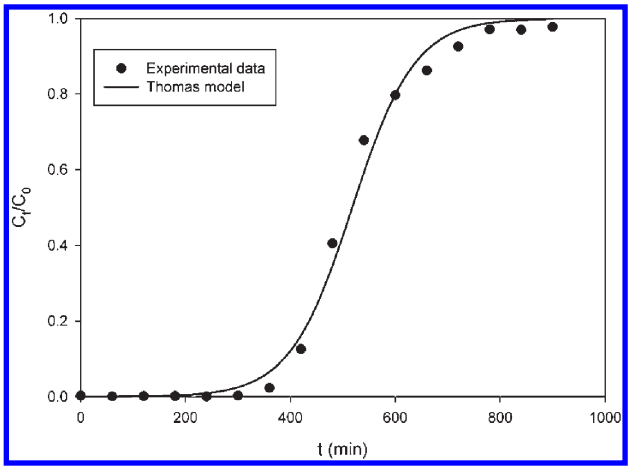

Figure 11. Experimental and predicted breakthrough curve of Cr(VI). The line represents the prediction using the Thomas model.

at 397.0 eV corresponding to certain interaction of amine from chitosan with the oxygen groups of composite materials. Whereas in the case of sample CCC-Cr, the new peak at 394.5 eV corresponds to less nitrogen protonated species; also the peaks at 392.5 eV suggest interaction of chromium ions as result of the chemical interaction of Cr(VI) with the functional groups in chitosan indicating a chemical reduction strongly bound the protonated amine sites. Chromate anions are sorbed in highly acidic solutions; chromate ions are known to be chemically reduced as this case.[10]

Figures 9a−c and 10a−c display the transition windows of C1s and O1s composites C, CCC, and CCC-Cr, respectively. Figure 9a could be fitted with five peaks, principally the most intensive due to C−C bonds and C−H carbon atoms. The peak close to 284.2 eV shown in Figure 9 corresponds to C−OH mostly from cellulose and peak at 286.1 eV appears most intensive as the chitosan is incorporated to composite, attributed to the presence of carbon in C−N and −C−O group. The peak near 282.5 and 280.3 eV seemed to be from reduced carbons in O−C−O of cellulose due to acidic treatment, and the peak at 288.2 eV was assigned to C═O from amide. In Figure 9c a new peak appears to the right after contact with the acidic solution; this seemed to be a carbon from the chitosan more reduced unto 278.1 eV that permits to form chelates the chromium with chitosan.

Figure 10 could be fitted with four O1s peaks and identified after deconvolution. The peak at 531.9 and 532.8 eV increases as the hydroxyl and acetyl group is incorporated, from (a) cellulose and (b) chitosan, respectively. Peak at 530.3 eV is assigned to the reduced oxygen from cellulose and HDPE when the composite is chemically treated before the incorporation of chitosan. Also in Figure 10b, intensity of peak 531.9 eV increases considerably due to exposure and interactions of −OH; furthermore peak at 527.0 eV is absent probably because of the coating of chitosan on the composite, which amended the pH on the surface. However, in Figure 10c of CCC-Cr, the peak at 527.0 eV increases significantly after metal contact with the adsorbent and supposes that oxygen has reduced again, first from cellulose and now from chitosan, attributed to addition of carbonyl group. This right peak indicates oxygen reductions mostly interact to form complexes when CCC interacts with the chromium solution.

In summary, the XPS analysis suggests that chromium ions interact with composite CCC, mainly through amino and hydroxyl groups from chitosan and/or cellulose from agave fiber. Cr(VI) can exist in several stable forms and the relative abundance of a

particular complex depends on the concentration of the chromium ion and the pH of the solution. In fact, the Cr(VI) reduces to Cr(III) as was observed by Boddu et al.[5] and Dambies et al.[10] The complexes formed during the interaction with chitosan and ions metals are able to be determined in a more detailed study, in the present work it can be concluded that chromium ions bind to chitosan and cellulose to form reduced species in some valence states.

3.7. Column Adsorption Experiments. The adsorption capacity of the material is greater when the process is carried out in a continuous system. Adsorption for these systems is a function of pH, initial concentration,[31] column dimensions, and the feed flow. Ideally the design of a system provides enough residence time to achieve the best adsorption. Runs were conducted with initial concentration of 99.7 mg L^{-1} and pH 6. The Thomas model was used to predict the adsorption process in the column

$$\frac{C_t}{C_0} = \frac{1}{1 + \exp[(k_{Th}/Q)(Q_0 M - C_0 V_t)]} \quad (6)$$

where C_0 is the initial concentration (inlet concentration) and C_t is the effluent concentration, Q is the flow rate, M is the mass of absorbent, V_t is the volume of treated effluent, and k_{Th} and Q_0 are the Thomas parameters, maximum solid phase concentration of Cr per unit of adsorbent mass and Thomas constant, respectively.[15]

Figure 11 shows an adsorption plot where the model is applied showing a good fit between experimental data and model. Values of k_{Th} = 0.1685 mL/(mg min) and Q_0 = 5.67 mg Cr/g adsorbent (or Q_0 = 171.3 mg Cr/g of chitosan) were obtained from nonlinear regression. For this adsorption the breakthrough point was reached at 300 min. In addition to the continuous experiments the minimum retention time within the column was determined to be 20 min.

4. CONCLUSIONS

There is a wide range of chitosan adsorption capacities reported in the literature; this study found that the prepared material has higher adsorption capacity compared to many of them. The adsorption capacity of Cr(VI) was observed to be dependent on both pH and initial concentration, with a greater adsorption capacity achieved at low pH and higher concentrations. The desorption experiments showed that the prepared material can only be regenerated using sulfuric acid. Continuous experimentation determined the minimum retention time in the column, which was 20 min. Finally, the high adsorption capacity presented by this material makes it suitable for the treatment of contaminated effluents.

■ ACKNOWLEDGMENT

Two of the authors (A.A. Perez-Fonseca and H. Davila) would like to thank the Mexican National Council for Science and Technology (CONACyT) for the scholarships.

■ AUTHOR INFORMATION

Corresponding Author

*E-mail: rubenglz@cencar.udg.mx.

■ REFERENCES

(1) Castro-Dantas, T. N.; Dantas-Neto, A. A.; Moura, M. C. P. A.; Barros-Neto, E. L.; Paiva- Telemaco, E. Chromium adsorption by chitosan impregnated with microemulsion. *Langmuir* **2001**, *17*, 4256–4260.

(2) Sag, Y.; Aktay, Y. Kinetic studies on sorption of Cr(VI) and Cu(II) ions by chitin, chitosan and *Rhizopus arrhizus*. *Biochem. Eng. J.* **2002**, *12* (2), 143–153.

(3) Hasan, S.; Krishnaiah, A.; Ghosh, T. K.; Viswanath, D. S.; Boddu, V. M.; Smith, E. D. Adsorption of chromium (VI) on chitosan-coated perlite. *Sep. Sci. Technol.* **2003**, *38* (15), 3775–3793.

(4) Bailey, S. E.; Olin, T. J.; Bricka, R. M.; Adrian, D. D. A review of potentially low-cost sorbents for heavy metals. *Water Res.* **1999**, *33*, 2469–2479.

(5) Boddu, V. M.; Abburi, K.; Talbott, J. L.; Smith, E. D. Removal of hexavalent chromium from wastewater using a new composite chitosan biosorbent. *Environ. Sci. Technol.* **2003**, *37*, 4449–4456.

(6) Minamisawa, M.; Minamisawa, H.; Yoshida, S.; Takai, N. Adsorption behavior of heavy metals on biomaterials. *J. Agric. Food Chem.* **2004**, *52*, 5606–5611.

(7) Park, S.; Jung, W. Y. Removal of chromium by activated carbon fibers plated with copper metal. *Carbon Sci.* **2001**, *2*, 15–21.

(8) Nomanbhay, S. M.; Palanisamy, K. Removal of heavy metal from industrial wastewater using chitosan coated oil palm shell charcoal. *Electron. J. Biotechnol.* **2005**, *8*, 43–53.

(9) Deans, J. R.; Dixon, B. G. Uptake of Pb^{2+} and Cu^{2+} by novel biopolymers. *Water Res.* **1992**, *26*, 469–472.

(10) Dambies, L.; Guimon, C.; Yiacoumi, S.; Guibal, E. Characterization of metal ion interactions with chitosan by X-ray photoelectron spectroscopy. *Colloids Surf. A* **2001**, *177*, 203–214.

(11) Varma, A. J.; Deshpande, S. V.; Kennedy, J. F. Metal complexation by chitosan and its derivatives: A review. *Carbohydr. Polym.* **2004**, *55*, 77–93.

(12) Inoue, K.; Yoshizuka, K.; Ohto, K. Adsorptive separation of some metal ions by complexing agent types of chemically modified chitosan. *Anal. Chim. Acta* **1999**, *388*, 209–218.

(13) Modrzejewska, Z; Kaminski, W. Separation of Cr (VI) on chitosan membranes. *Ind. Eng. Chem. Res.* **1999**, *38*, 4946–4950.

(14) Guibal, E. Heterogeneous catalysis on chitosan-based materials: A review. *Prog. Polym. Sci.* **2005**, *30*, 71–109.

(15) Morales, F. C.; Kanb, C.; Dalidac, M. L.; Pascuad, C.; Wanb, M. W. Fixed-bed column studies on the removal of copper using chitosan immobilized on bentonite. *Carbohydr. Polym.* **2011**, *83*, 697–704.

(16) Wan-Ngah, W. S.; Teong, L. C.; Hanafiah, M. A. K. M. Adsorption of dyes and heavy metal ions by chitosan composites: A review. *Carbohydr. Polym.* **2011**, *83*, 1446–1456.

(17) Vázquez, M. O.; Herrera, V. S.; Gómez, C.; Gómez-Salazar, S.; Rodrigue, D.; González-Núñez, R.; Luna-Barcenas, J. G.; Mani-González, P. G.; Herrera-Gomez, A. Postconsumer high-density polyethylene/agave fiber foamed composites coated with chitosan for the removal of heavy metals. *J. Appl. Polym. Sci.* **2010**, *115*, 2971–2980.

(18) Samecka-Cymerman, A.; Kempers, A. J. Heavy metals in aquatic macrophytes from two small agricultural and textile industry sewages SW Poland. *Arch. Environ. Contam. Toxicol.* **2007**, *53*, 198–206.

(19) Zereen, F.; Islam, F.; Habib, M. A.; Begum, D. A.; Zaman, M. S. Inorganic pollutants in the Padma River, Bangladesh. *Environ. Geol.* **1999**, *39*, 1059–1052.

(20) Eaton, A. D.; Franson, M. A. H. *Standard Methods for the Examination of Water and Wastewater*; American Public Health Association: Washington, DC, 2005.

(21) Stark, N.; Matuana, L. M. Characterization of weathered wood-plastic composite surfaces using FTIR spectroscopy, contact angle, and XPS. *Polym. Degrad. Stab.* **2007**, *92*, 1883–1890.

(22) Jin, L.; Bai, R. B. Mechanisms of lead adsorption on chitosan/PVA hydrogel beads. *Langmuir* **2002**, *18*, 9765–9770.

(23) Rana, M. S.; Halim, M. A.; Safiullah, S.; Mamun, M. M.; Azam, M. S.; Goni, M. A.; Kamal, H. M.; Rana, M. M. Removal of Heavy Metal from Contaminated Water by Biopolymer Crab Shell Chitosan. *J. Appl. Sci.* **2009**, *9*, 2762–2769.

(24) Vicent, T.; Guibal, E. Cr(VI) Extraction Using Aliquat 336 in a Hollow Fiber Module Made of Chitosan. *Ind. Eng. Chem. Res.* **2001**, *40*, 1406–1411.

(25) Guibal, E. Interactions of metal ions with chitosan-based sorbents: A review. *Sep. Purif. Technol.* **2004**, *38*, 43–74.

(26) Pérez, C. M.; Martín, M. J M.; Torrengrosa, M. R. Chromium (VI) removal with activated carbons. *Water Res.* **1995**, *29*, 2174–2180.

(27) Sankararamakrishnan, N.; Dixit, A.; Iyengar, L.; Sanghi, R. Removal of hexavalent chromium using a novel cross linked xanthated chitosan. *Bioresour. Technol.* **2006**, *97*, 2377–2382.

(28) Lee, S. T.; Mi, F. L.; Shen, Y. J.; Shyu, S. S. Equilibrium and kinetic studies of copper(II) ion uptake by chitosan-tripolyphosphate chelating resin. *Polymer* **2001**, *42*, 1879–1892.

(29) Aydin, Y. A.; Aksoy, N. D. Adsorption of chromium on chitosan: Optimization, kinetics and thermodynamics. *Chem. Eng. J.* **2009**, *151*, 188–194.

(30) Agulló, E.; Mato, R.; Peniche, C.; Tapia, C.; Heras, A.; San Román, J.; Argüelles, W.; Goycoolea, F.; Mayorga, A.; Nakamatsu, J.; Pastor de Abram, A. *Quitina y Quitosano: Caracterización y aplicaciones*; Pontificia Universidad Católica del Perú, Fondo Ed.ial, 2004.

(31) Xu, Y.; Zhang, J.; Qian, G.; Ren, Z.; Xu, Z. P.; Wu, Y.; Liu, Q.; Qiao, S. Effective Cr(VI) removal from simulated groundwater through hydrotalcite-derived adsorbent. *Ind. Eng. Chem. Res.* **2010**, *49*, 2752–2758.